



# On the accuracy of laminar flame speeds measured from outwardly propagating spherical flames: Methane/air at normal temperature and pressure



Zheng Chen

SKLTCs, Department of Mechanics and Engineering Science, College of Engineering, Peking University, Beijing 100871, China

## ARTICLE INFO

### Article history:

Received 17 January 2015

Received in revised form 13 February 2015

Accepted 13 February 2015

Available online 11 March 2015

### Keywords:

Laminar flame speed

Propagating spherical flame

Methane/air

Uncertainty

## ABSTRACT

The present work investigates the accuracy of laminar flame speeds measured from outwardly propagating spherical flames. We focus on methane/air mixtures at normal temperature and pressure, for which there is a variety of data sets reported in the literature. It is observed that there are large discrepancies in laminar flame speed measurement, which makes these experimental data unhelpful for restraining the uncertainty of chemical models. Different sources of uncertainty/inaccuracy (including mixture preparation, ignition, buoyancy, instability, confinement, radiation, nonlinear stretch behavior, and extrapolation) are discussed and their contributions to large discrepancies in laminar flame speed measurement are assessed with the help of 1-D simulation. It is found that the uncertainty in equivalence ratio can bring large inconsistency in laminar flame speed measurement, especially for off-stoichiometric mixtures and experiments using pressure gauge with normal or low accuracy. For fuel-rich methane/air mixtures, the large deviations in laminar flame speed measurement could be partly caused by nonlinear stretch behavior and extrapolation. The change of the influence of different sources of uncertainty with initial pressure, initial temperature, and fuel carbon number is also discussed. Furthermore, it is shown that the discrepancy in raw experimental data can be possibly hidden after extrapolation is conducted. Therefore, the data used for extrapolation as well as extracted results should be reported and compared with simulation or other experiments. The recommendations on the laminar flame speeds measurement using the propagating spherical flames are also provided.

© 2015 The Combustion Institute. Published by Elsevier Inc. All rights reserved.

## 1. Introduction

The laminar flame speed,  $S_u^0$ , is defined as the speed at which a planar, unstretched, adiabatic, premixed flame propagates relative to the unburned gas [1]. It is an important parameter of a combustible mixture since it determines the fuel burning rate and flame stabilization in practical combustors. On a more fundamental level,  $S_u^0$  is an important target for validating chemical mechanisms and for developing surrogate fuel models (e.g., [2–7]). Various experimental approaches have been developed to measure  $S_u^0$  using different flame configurations such as Bunsen flame, flat-burner flame, counterflow/stagnation flame, and outwardly propagating spherical flame (OPF) [1,5]. The advantages and limitations of these approaches have been recently reviewed by Egolfopoulos et al. [5]. Currently, due to the simple flame configuration and well-defined stretch rate, the OPF method is popularly used to measure  $S_u^0$ , especially at high pressures.

Accurate measurement of laminar flame speed is extremely important since the sensitivity of  $S_u^0$  to chemical kinetics is relatively low [5]. It is very difficult to constrain the uncertainty of chemical models using low-quality (with large-uncertainty) experimental data of  $S_u^0$  [5,8]. Recently, substantial attention has been devoted to improving the accuracy of laminar flame speed measurement using the OPF method ([5] and references therein). For example, a collaborative study has been initiated to investigate the potential error sources and to reduce the uncertainty associated with  $S_u^0$  measurement [9]. For large molecular weight fuels or liquid fuels, the uncertainty associated with  $S_u^0$  measurement using the OPF method can be large due to the effects of molecular transport (differential diffusion of reactants) [10] and/or fuel heating and vaporization [5,9]. For small molecular weight gaseous fuels (such as methane and propane, not including hydrogen), the uncertainty in  $S_u^0$  measurements is usually considered to be small, at least for conditions at normal temperature and pressure (NTP,  $T_u = 298$  K,  $P = 1$  atm). A new experimental setup for  $S_u^0$  measurement is usually

E-mail address: [cz@pku.edu.cn](mailto:cz@pku.edu.cn)

validated against experimental data for CH<sub>4</sub>/air at NTP reported in the literature.

However, as will be shown in this study (see Figs. 1 and 3), the discrepancies in  $S_u^0$  measured for CH<sub>4</sub>/air at NTP using the OPF method still remain substantial – often exceeding typical quoted uncertainties in the measurements. These persistent discrepancies among experimental data themselves make it difficult to interpret comparisons between experimental data and model predictions in kinetic mechanism validation [8]. In order to reduce the discrepancies in  $S_u^0$  measurements, the possible sources of uncertainty should be investigated. Besides, information on the uncertainty in  $S_u^0$  measured in experiments is also important for kinetic model validation and optimization [11,12].

The objectives of the present work are (1) to identify the discrepancies in  $S_u^0$  measured for CH<sub>4</sub>/air at NTP using the same OPF method by different groups; and (2) to investigate possible sources of uncertainty/inaccuracy in  $S_u^0$  measurements. Specifically, a variety of experimental data sets for CH<sub>4</sub>/air reported in the literature [13–26] is collected to show the differences in  $S_u^0$  measurement using the OPF method. Moreover, effects of mixture preparation [5,9,27,28], ignition [29–32], buoyancy [33,34], instability [35–37], confinement [38–41], radiation [9,10,41–44], nonlinear stretch behavior [22,45–49], and extrapolation [50,51] on the discrepancies in  $S_u^0$  measurement are examined based on 1-D simulation of propagating planar and spherical flames. It should be noted that Egolfopoulos et al. [5] have recently reviewed possible sources of uncertainty in  $S_u^0$  measurement using the OPF method. However, in that study the contributions of individual source of uncertainty have not been assessed/quantified specifically for CH<sub>4</sub>/air.

The paper is organized as follows: in Section 2, the OPF method and numerical method are briefly described; then, in Section 3, discrepancies in  $S_u^0$  measured by different groups for CH<sub>4</sub>/air at NTP are presented; possible sources of uncertainty in  $S_u^0$  measurement using the OPF method are discussed in Section 4, after which additional notes and recommendations are respectively presented in Sections 5 and 6; and finally, the conclusions are summarized in Section 7.

## 2. Methodologies

Depending on the combustion chamber design and pressure rise, there are two different methods for  $S_u^0$  measurement using OPF: the constant-pressure method (e.g., [13–26]) and the constant-volume method (e.g., [52–54]). Only the constant-pressure OPF method is considered here and hereafter it is simply called OPF method. In this method, a confined chamber or a pressure-release dual-chamber is used in experiments. The flame front history of OPF,  $R_f = R_f(t)$ , is recorded by high-speed schlieren or shadowgraphy. Usually, the burned gas inside the spherical flame is assumed to be static and thus the stretched flame speed relative to burned gas is  $S_b = dR_f/dt$ . The unstretched laminar flame speed,  $S_b^0$ , together with the Markstein length,  $L_b$ , both relative to burned gas, can be obtained from extrapolation based on the following linear model:

$$S_b = S_b^0 - L_b K \quad (1)$$

where  $K = (2/R_f)(dR_f/dt)$  is the stretch rate for OPF. Knowing  $S_b^0$ ,  $S_u^0$  can be determined through  $S_u^0 = \sigma S_b^0$ , where  $\sigma = \rho_b/\rho_u$  is the density ratio between burned gas (at equilibrium condition) and unburned gas.

When Eq. (1) is used, numerical differentiation needs to be conducted to get  $S_b$  and  $K$ . This can be avoided by integrating Eq. (1) which yields the following expression:

$$S_b t = S_b^0 t - 2L_b \ln(R_f) + \text{const} \quad (2)$$

Besides the linear model, the following nonlinear model was proposed by Kelley and Law [45] in the extraction of  $S_b^0$  and  $L_b$ :

$$\left(\frac{S_b}{S_b^0}\right) \ln\left(\frac{S_b}{S_b^0}\right) = -\frac{2L_b}{R_f} \quad (3)$$

This model is based on the quasi-steady, adiabatic form of the relation first derived by Ronney and Sivashinsky [55]. The accuracy and performance of the nonlinear model were discussed in [22,45–47].

This paper summarizes the experimental data for CH<sub>4</sub>/air at NTP from previous studies [13–26] which measured  $S_u^0$  using the OPF method. The details on initial temperature and pressure, equivalence ratio range, extrapolation model, and chamber geometry are summarized in Table 1 (Most of data sets in the table were reported in the last ten years).

In order to isolate and assess the contribution of individual source of uncertainty, 1-D simulation of propagating planar and spherical flames is conducted. Detailed chemistry for methane oxidation, GRI-Mech. 3.0 [56], is used in simulation. The unstretched, adiabatic, freely-propagating planar flame is simulated using CHEMKIN-PREMIX code [57] to get  $S_u^0$  and  $\sigma$ . The number of grid points is kept to be above 700 so that the calculated laminar flame speed and density ratio is grid-independent. OPF is simulated using A-SURF [31,41], which solves the conservation equations of one-dimensional, multi-component, reactive flow in a spherical coordinate using the finite volume method. The CHEMKIN packages [58] are incorporated into A-SURF to calculate the temperature- and component-dependent thermodynamic and transport properties. Detailed chemistry is efficiently handled in A-SURF with the help of algorithms introduced in [59,60]. A-SURF has been successfully used in previous studies on ignition and flame propagation (e.g., [61–64]). The details on governing equations, numerical schemes, and code validation can be found in [31,41]. To adequately resolve the moving flame front, a multi-level, dynamically adaptive mesh with finest mesh size of 8  $\mu\text{m}$  is used. Unless otherwise stated, a large chamber radius of  $R_w = 100$  cm is used (to ensure the confinement effect is negligible) and adiabatic condition is considered (to eliminate the radiation effect).

## 3. Discrepancies in $S_u^0$ measured for CH<sub>4</sub>/air at NTP

The laminar flame speeds of CH<sub>4</sub>/air at NTP measured by different groups [13–26] (see Table 1) are plotted in Fig. 1. The prediction from GRI-Mech. 3.0 [56] is also shown for comparison. All the experimental results (symbols in Fig. 1) were measured using the OPF method. Lower scatter is observed for stoichiometric mixture, and higher scatter is observed for off-stoichiometric mixtures. Even for near-stoichiometric mixture of  $\phi = 0.9$ , high scatter is observed. It is noticed that  $S_u^0$  measured near the lean flammability limit by Wang et al. [23] is much lower than prediction from GRI-Mech. 3.0. This is not caused by buoyancy effect since Wang et al. [23] conducted experiments at  $10^{-3}$ – $10^{-2}$  g reduced gravity. It is the radiation and compression effects that make reported  $S_u^0$  much lower than its correct value [41].

The Markstein lengths of CH<sub>4</sub>/air at NTP measured using the OPF method are shown in Fig. 2. Compared to  $S_u^0$ , the discrepancies in  $L_b$  are shown to be much larger. The relative difference can even be above 300% under fuel-rich conditions. This is due to the facts that  $L_b$  measurement is very sensitive to extrapolation and that the uncertainty in  $L_b$  is about one-order larger than that in  $S_u^0$  [46]. Significant effort needs to be devoted to improving the

**Table 1**  
Previous experimental studies [13–26] on laminar flame speed measurement of CH<sub>4</sub>/air at NTP using the OPF method.

No.	$T_u$ (K)	$P$	$\phi$	Extrapolation model	Data used in extrapolation <sup>a</sup>	Chamber <sup>b</sup>	Notes	1st Author, year, Ref.
1	293–299	1 atm	0.55–1.4	Eq. (2)	$R_f < 3.5$ cm	Spherical, $R_w = 30$ cm	N1	Taylor, 1991 [13]
2	298 ± 3	1 atm	0.6–1.35	Eq. (1)	$R_f < 3$ cm	Quasi-spherical, $R_w = 13$ cm	N1, N4	Aung, 1995 [14]
3	298	1 atm	0.6–1.3	Eq. (1)	$0.5 \leq R_f \leq 3$ cm	Spherical, $R_w = 18$ cm	N1, N4	Hassan, 1998 [15]
4	300–302	0.1 MPa	0.6–1.2	Eq. (1)	$R_f > 0.6$ cm	Spherical, $R_w = 19$ cm	N1	Gu, 2000 [16]
5	298	1 atm	0.6–1.3	Eq. (2)	$0.5 \leq R_f \leq 2$ cm	Cylindrical, $R_w = 4.128$ cm, $L = 12.7$ cm	N2, N5	Rozenchan, 2002 [17]
6	298	1 atm	0.67–1.35	Eq. (2)	$1.0 \leq R_f \leq 2.5$ cm	Cylindrical, $R_w = 5$ cm, $L = 15.24$ cm	N3, N5	Qin, 2005 [18]
7	298	0.1 MPa	0.7–1.2	Eq. (1)	$0.5 \leq R_f \leq 3$ cm	Spherical, $R_w = 12.5$ cm	N2	Halter, 2005 [19]
8	303	0.1 MPa	0.6–1.3	Eq. (1)	$0.5 \leq R_f \leq 2.5$ cm	Cylindrical, $R_w = 9$ cm, $L = 21.6$ cm	N3	Hu, 2009 [20]
9	300 ± 3	0.1 MPa	0.55–1.3	Eq. (1)	$0.7 \leq R_f \leq 3$ cm	Cylindrical, $R_w = 16$ cm, $L = 30$ cm	N1, N6	Tahtouh, 2009 [21]
10	300	0.1 MPa	0.6–1.3	Eq. (3)	$0.8 \leq R_f \leq 2.7$ cm	Cylindrical, $R_w = 16$ cm, $L = 30$ cm	N2	Halter, 2010 [22]
11	298 ± 2	1 atm	0.51–0.6	Eq. (1)	$R_f > 1.1$ –1.5 cm	Cubic, $L = 8$ cm	N1, N7	Wang, 2010 [23]
12	293–296	1 atm	0.7–1.3	Eq. (2)	$0.7 \leq R_f \leq 4.5$ cm	Cylindrical, $R_w = 15.25$ cm, $L = 35.6$ cm	N1	Lowry, 2011 [24]
13	298	0.1 MPa	0.6–1.3	Eqs. (1), (3)	$0.65 \leq R_f \leq 1.9$ cm	Spherical, $R_w = 8.5$ cm	N2	Varea, 2012 [25]
14	298–300	1 atm	0.6–1.3	Eq. (3)	$R_f > 0.25$ cm	Spherical, $R_w = 5$ cm	N2, N8	Beeckmann, 2014 [26]

Notes:

N1: The laminar flame speed data were from table in this paper.

N2: The laminar flame speed data were extracted from graph in this paper.

N3: The laminar flame speed data were supplied by the first author of this paper.

N4: Different form of model Eq. (1). See Ref. [14] for details.

N5: Pressure-release dual-chamber; only the size of the inner cylinder is described.

N6: A new method based on analytical solution of Eq. (1) was proposed for data processing. See Ref. [21] for details.

N7: Experiments were conducted at micro-gravity condition (free-fall facility experiencing 1.2 s of  $10^{-3}$ – $10^{-2}$  g reduced gravity).

N8: Experiments were performed with technical air (O<sub>2</sub>:N<sub>2</sub> = 20.5:79.5 vol.) and the data were scaled to real air conditions with O<sub>2</sub>:N<sub>2</sub> = 20.94:79.06.

<sup>a</sup> The flame radius range usually changes with equivalence ratio and it could be narrower than (but within) the one listed in the table.

<sup>b</sup>  $R_w$  is the inner radius for the spherical or cylindrical chamber and  $L$  is the length of cylindrical or cubic chamber.

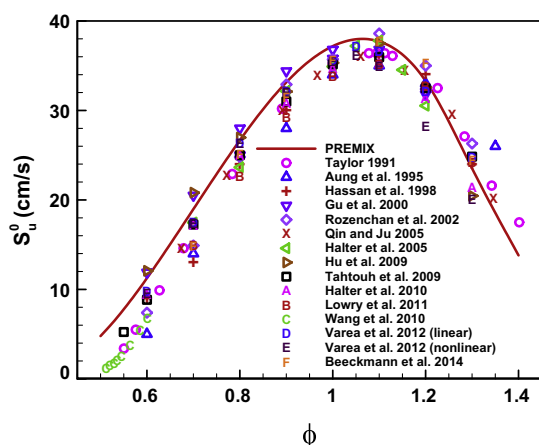


**Fig. 1.** Laminar flame speed of CH<sub>4</sub>/air at NTP. The symbols denote experimental results measured from OPF [13–26] (see details listed in Table 1). The line denotes numerical results predicted by GRI-Mech. 3.0 [56] using CHEMKIN-PREMIX code [57].

accuracy of  $L_b$  measurement in the future. The present work only focuses on  $S_u^0$  measurement using the OPF method.

To quantify the discrepancies in  $S_u^0$  measured from OPF, Fig. 3 shows the deviation of  $S_u^0$  measured by different groups [13–22,24–26] from that predicted by simulation,  $S_{u,PREMIX}^0$ , based on GRI-Mech. 3.0 [56]. The near-lean-flammability limit data of Wang et al. [23] are not included in Fig. 3 since they are greatly affected by radiation and compression effects [41]. For stoichiometric mixture, the difference among normalized values of  $S_u^0/S_{u,PREMIX}^0$  is the smallest but still reaches 7.6%. For very lean and rich cases, the maximum difference is notably greater: it is 40.6% and 26.4% for  $\phi = 0.6$  and  $\phi = 1.3$ , respectively. Even for  $\phi = 0.9$ , the maximum difference reaches around 20%. In terms of absolute value, Fig. 3(b) indicates that the differences among  $S_u^0$  measured by different groups are above 5 cm/s for the majority of equivalence ratios and can reach 8 cm/s for  $\phi = 0.7$ . Therefore, the variety of data sets

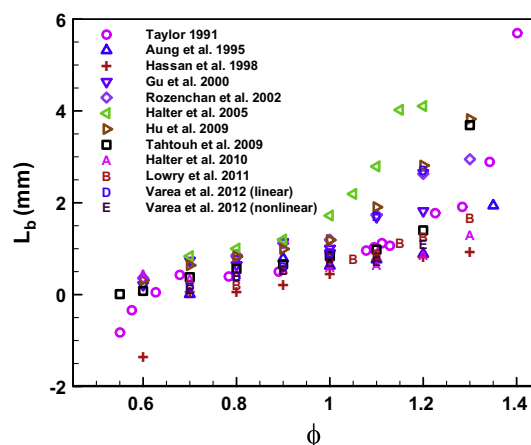


**Fig. 2.** Markstein length relative to burned gas for CH<sub>4</sub>/air at NTP measured from OPF.

in Fig. 3 demonstrates that even for CH<sub>4</sub>/air at NTP, there are large discrepancies in  $S_u^0$  measured using the OPF method. In the recent review paper of Egolfopoulos et al. [5], it was stated that “the resulting uncertainty in  $S_u^0$  measurements in spherical flames is about 5%. In extreme cases... the uncertainty can be significantly greater.” and “differences (in  $S_u^0$ ) of the order of 3–5 cm/s persist for low molecular weight fuels such as C1–C4 hydrocarbons”. The present results show that the discrepancies in  $S_u^0$  measurement using the OPF method exceed what appear to be commonly expected. Efforts still need to be devoted to improving the accuracy of  $S_u^0$  measured using the OPF method.

Sensitivity of  $S_u^0$  to the rate of  $k^{\text{th}}$  elementary reaction,  $S_K$ , is shown in Fig. 4(a). The sensitivity is defined as  $S_K = \partial \ln(S_u^0) / \partial \ln(A_k)$ , in which  $A_k$  is the A-factor of the rate of  $k^{\text{th}}$  elementary reaction [57]. As mentioned in [5], low sensitivity of  $S_u^0$  to chemical kinetics is observed. Moreover, the most sensitive elementary reaction R38

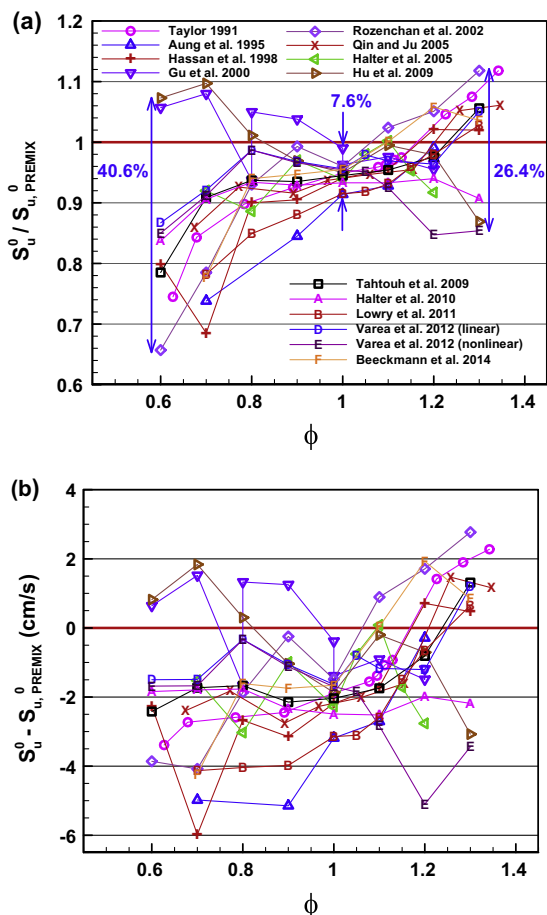


**Fig. 3.** Deviation of  $S_u^0$  measured by different groups [13–22,24–26] from that predicted by simulation,  $S_{u,PREMIX}^0$  based on GRI-Mech. 3.0 [56].

( $H + O_2 = O + OH$ ) is well studied and it has very low uncertainty. In kinetics validation, not only the sensitivity but also the uncertainty in elementary reaction rate is important. Following Santner et al. [27], the sensitivity-weighted uncertainty momentum is used here and it is defined as  $\delta_K = S_K \times (f_K - 1)$ . In this expression,  $f_K$  is the uncertainty factor of  $k^{\text{th}}$  elementary reaction as described by Sheen et al. [65] ( $f_K = 1.2$  for R35, R36, R38, and R99;  $f_K = 2.0$  for R119;  $f_K = 4.0$  for R52). As the rate coefficient uncertainty diminishes (i.e.  $f_K \rightarrow 1$ ), the sensitivity-weighted uncertainty moment vanishes (i.e.  $\delta_K \rightarrow 0$ ) [27]. Figure 4(b) shows that  $\delta_K$  of sensitive reactions is within 20%. One exception is R52 ( $CH_3 + H + M = CH_4 + M$ ), for which  $\delta_K$  is above 40% at  $\phi > 1.1$ . This is because a very large uncertainty factor of  $f_K = 4.0$  [65] is used for R52. According to more recent uncertainty quantification, the uncertainty factor for R52 is less than 2.0 [66] and thereby  $\delta_K$  of R52 is at most one-third of the value shown in Fig. 4(b). It is observed that the magnitudes of  $\delta_K$  of the most important elementary reactions, R38 ( $H + O_2 = O + OH$ ) and R99 ( $CO + OH = H + CO_2$ ), are much smaller than the discrepancies in  $S_u^0$  measurement shown in Fig. 3(a). This also holds for other elementary reactions except R52. Therefore, as also mentioned in [5],  $S_u^0$  data with large discrepancies are unhelpful for restraining the uncertainty of chemical models and thereby high-quality experimental data of  $S_u^0$  are needed.

#### 4. Possible sources of uncertainty

In the following, we shall investigate possible sources of uncertainty in  $S_u^0$  measured for  $CH_4/air$  at NTP using the OPF method.

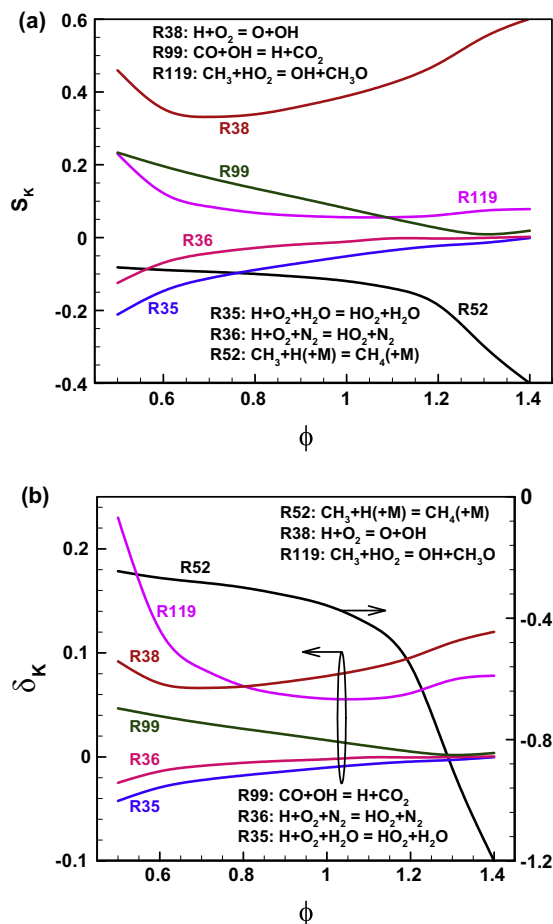


**Fig. 4.** (a) Sensitivity coefficient,  $S_K$ , and (b) sensitivity-weighted uncertainty momentum,  $\delta_K$ , as a function of equivalence ratio for laminar flame speed of  $CH_4/air$  at NTP.  $\delta_K = S_K \times (f_K - 1)$  [27] and  $f_K$  is the uncertainty factor of  $k^{\text{th}}$  elementary reaction ( $f_K = 1.2$  for R35, R36, R38, and R99;  $f_K = 2.0$  for R119;  $f_K = 4.0$  for R52) [65].

These sources include mixture preparation [5,9,27,28], ignition [29–32], buoyancy [33,34], instability [35–37], confinement [38–41], radiation [9,10,41–44], nonlinear stretch behavior [22,45–49], and extrapolation [50,51]. The references cited above provide information or details about the effects of each source on  $S_u^0$  measured using the OPF method. Simulation is conducted since it has the advantage that different sources of uncertainty can be isolated and examined individually. Unless otherwise stated, the results in figures presented in this section are from or based on simulation.

##### 4.1. Mixture preparation

The laminar flame speed depends on experimental conditions for initial temperature,  $T_u$ , pressure,  $P$ , and equivalence ratio,  $\phi$ . The small difference in  $T_u$ ,  $P$ , and/or  $\phi$  during initial mixture preparation might induce discrepancies in  $S_u^0$  measurement. Table 1 shows that the initial temperature and pressure are not exactly the same as those at NTP ( $T_u = 298$  K,  $P = 1$  atm). The influence of small perturbation of  $T_u$  or  $P$  on  $S_u^0$  is demonstrated in Fig. 5(a). It is observed that the relative change in  $S_u^0$  is around  $\pm 2\%$  when  $T_u$  is perturbed by  $\pm 3$  K from  $T_u = 298$  K and it is  $\pm 2.5$ – $4\%$  for  $\Delta T_u = \pm 5$  K. The influence of  $T_u$  slightly increases away from  $\phi = 1.0$ . Table 1 shows that some groups conducted experiments at  $P = 0.1$  MPa instead of  $P = 1$  atm. This slight change in pressure brings about 0.6% relative increase in  $S_u^0$  according to Fig. 5(a).

Compared to  $T_u$  and  $P$ , the uncertainty in  $\phi$  brings much larger change in  $S_u^0$  under fuel-lean and fuel-rich conditions. Figure 5(b) indicates when the equivalence ratio is changed by  $\pm 0.01$  in absolute value or  $\pm 1\%$  relatively, the relative change in  $S_u^0$  can reach  $\pm 4\text{--}7\%$  for  $\phi = 0.6$  and  $\phi = 1.4$ . For near-stoichiometric mixtures with  $0.8 \leq \phi \leq 1.2$ , the relative change in  $S_u^0$  becomes smaller (within  $\pm 3\%$ ).

Beeckmann et al. [9] mentioned that in OPF experiments conducted by different groups, the uncertainty in  $\phi$  is less than 0.01 in absolute value or 0.8% in relative value. Egolfopoulos et al. [5] mentioned that the uncertainty in  $\phi$  for  $\text{CH}_4/\text{air}$  increases away

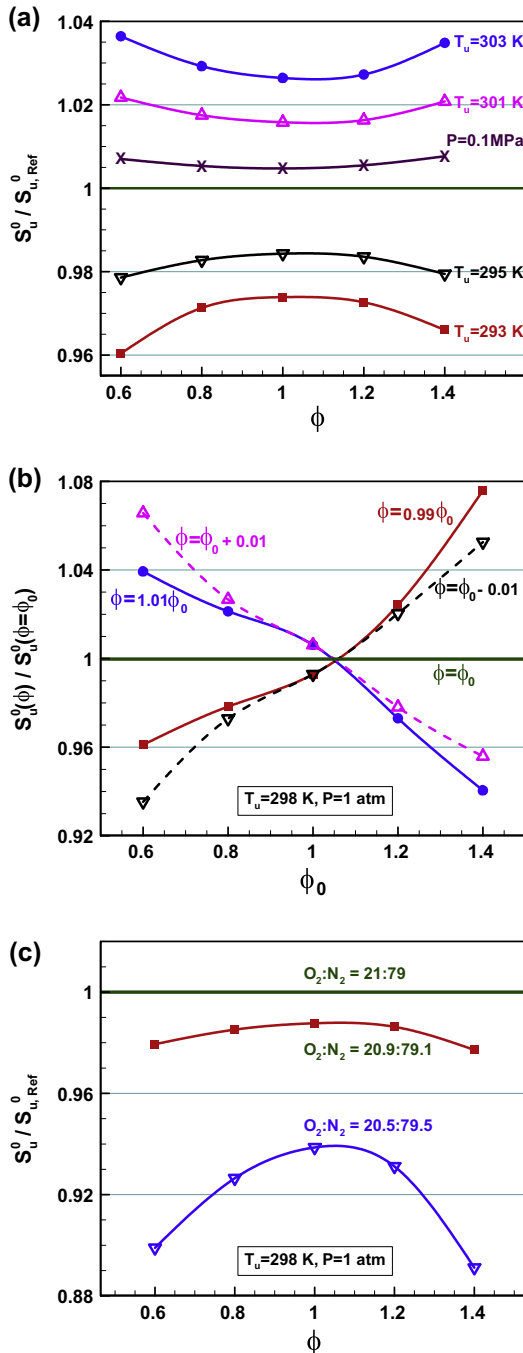


Fig. 5. Effects of (a) initial temperature and pressure, (b) equivalence ratio, and (c) oxygen/nitrogen ratio on the laminar flame speed of  $\text{CH}_4/\text{air}$  at NTP.  $S_{u,\text{Ref}}^0$  is the laminar flame speed at reference state of  $T_u = 298 \text{ K}$ ,  $P = 1 \text{ atm}$ , and  $\text{O}_2:\text{N}_2 = 21:79$  (vol.) and it is calculated using CHEMKIN-PREMIX code.

from  $\phi = 1.0$  and it is around 0.005 and 0.035 for  $\phi = 0.7$  and  $\phi = 1.4$ , respectively. Partial pressure method is usually used to prepare the mixture in OPF experiments. The uncertainty in mixture composition depends on the accuracy of pressure gauge used in experiments. For alkane ( $\text{C}_n\text{H}_{2n+2}$ ) and air mixture prepared for the objective equivalence ratio of  $\phi_0$  and at the pressure of  $P$ , the real equivalence ratio is

$$\phi = \phi_0 + \left( \frac{\Delta P_{\text{Fuel}}}{P} - \frac{\phi_0}{1.5n+0.5} \frac{\Delta P_{\text{O}_2}}{P} \right) [\phi_0 + (1.5n+0.5)(1+r)] \quad (4)$$

where  $\Delta P_{\text{Fuel}}$  and  $\Delta P_{\text{O}_2}$  are the uncertainties in partial pressure of fuel and oxygen, respectively, and  $r$  is the nitrogen/oxygen molar ratio in air (e.g.  $r = 0.79/0.21$ ). When a high accuracy digital pressure gauge with  $\pm 0.05\%$  full-scale (15 psi) accuracy is used, the uncertainty in  $\phi$  for  $\text{CH}_4/\text{air}$  at  $P = 1 \text{ atm}$  is 0.65–1.15% (Fig. 6). This brings about 6% discrepancy in  $S_u^0$  for  $\phi = 0.6$  and  $\phi = 1.4$  according to Fig. 5(b). For pressure gauge with normal accuracy of  $\pm 0.25\%$  (which might be commonly used in OPF experiments), the uncertainty in  $\phi$  increases roughly by a factor of five and so does the deviation in  $S_u^0$ . Therefore, for off-stoichiometric mixtures with  $\phi = 0.6$  and  $\phi = 1.4$ , significant discrepancy in  $S_u^0$  might be caused by uncertainty in  $\phi$ . This also happens to near-stoichiometric mixtures with  $\phi = 0.8$  and  $\phi = 1.2$  when pressure gauge with normal or low accuracy is used in experiments.

It is noted that according to Eq. (4), the uncertainty in  $\phi$  is nearly proportional to carbon number  $n$ . Therefore, when the OPF method is used for large hydrocarbon fuels, the uncertainty in  $S_u^0$  caused by mixture composition is significant. This might help to explain the large discrepancy in  $S_u^0$  of  $\text{iC}_8\text{H}_{18}/\text{air}$  measured by two groups using the same OPF method [67].

The laminar flame speed also depends on the ratio between oxygen and nitrogen. According to Fig. 5(c),  $S_u^0$  is reduced by 6–11% when the oxygen volumetric fraction is changed from 21% to 20.5%. Therefore, the difference in air composition or oxygen/nitrogen ratio can also bring large discrepancy in  $S_u^0$  measurement using the OPF method. For fair comparison, proper re-scaling should be conducted for  $S_u^0$  measured at different oxygen/nitrogen ratios [26].

#### 4.2. Ignition

In the OPF method, a proper flame radius range,  $[R_{fL}, R_{fU}]$ , is chosen during data processing. Usually, the lower radius bound,  $R_{fL}$ , is chosen to reduce the influence of ignition and nonlinear stretch

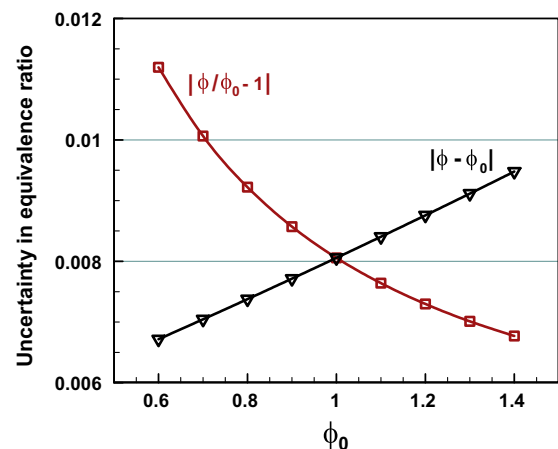


Fig. 6. The uncertainty in equivalence ratio for  $\text{CH}_4/\text{air}$  at  $P = 1 \text{ atm}$  when the accuracy of pressure gauge is  $\pm 0.05\%$  full-scale (15 psi).

behavior; and the upper bound,  $R_{fl}$ , is chosen to reduce the influences of buoyancy, flame instability, confinement, and radiation.

Theory [31,68–71], simulation [29,31,72], and experiments [31,45] all shows that OPF is affected by ignition energy when the flame radius is small. Based on their simulation of stoichiometric CH<sub>4</sub>/air flames, Bradley et al. [29] suggested that  $R_{fl} = 6$  mm is appropriate to eliminate the ignition effect. This suggestion was taken by many other researchers using the OPF method. For CH<sub>4</sub>/air mixtures, the Markstein length increases with equivalence ratio (see Fig. 2) and so does the ignition effect [31]. Figure 7 shows that the flame speed trajectory become nearly independent of the ignition energy at  $R_f \geq 4$  mm for  $\phi = 0.8$  and at  $R_f \geq 8$  mm for  $\phi = 1.4$ . It should be mentioned that large ignition energies (more than five times of the minimum ignition energy, MIE) are used in simulation to exaggerate the ignition effect. In OPF experiments, low ignition energy close to the MIE is usually chosen to reduce the ignition effect. Therefore, for CH<sub>4</sub>/air mixtures at NTP,  $R_{fl} = 6$  mm can be chosen such that the ignition effect on  $S_u^0$  measurement using the OPF method is negligible.

It should be emphasized that for mixtures with large Lewis number (e.g., rich H<sub>2</sub>/air) [31] or at sub-atmospheric condition, the ignition effect becomes stronger. Therefore, a larger value of  $R_{fl}$  above 6 mm should be chosen so that the ignition effect can be eliminated. It is noted that experimental data for spherical flames with small radii (e.g.  $R_f < 5$  mm) are helpful for understanding flame propagation properties in meso-scale with high stretch rate though they cannot be used to extrapolate the laminar flame speed. For example, Nakahara et al. [73,74] studied the meso-scale propagating spherical flames for different fuels and found that the stretched flame speed changes non-monotonically with flame radius (or stretch rate).

### 4.3. Buoyancy

Experiments for OPF are usually conducted at normal gravity. For slow-burning mixtures (near the flammability limits or highly-diluted), the spherical flame propagation in normal gravity is strongly affected by buoyancy and thereby experiments in

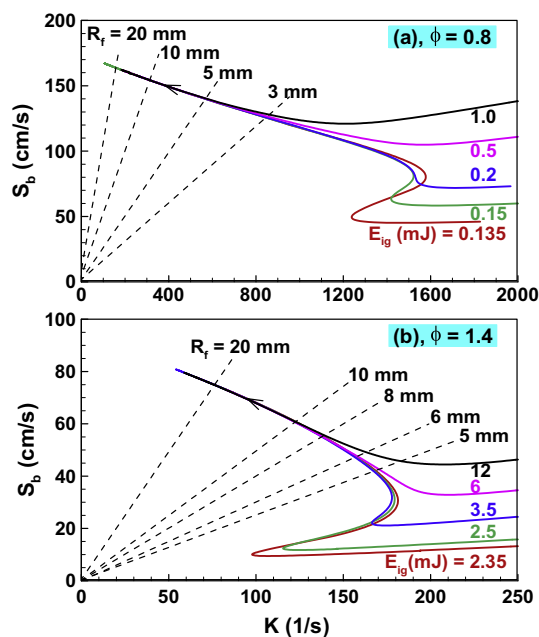


Fig. 7. Effect of ignition energy on the propagation of spherical CH<sub>4</sub>/air flames at NTP. The dashed lines denote the flame radii contours (they are straight lines since  $R_f = 2S_b/K$ ).

microgravity become essential for  $S_u^0$  measurement using the OPF method [33,34]. A short-drop free-fall microgravity facility was developed by Qiao et al. [34,75,76] to measure  $S_u^0$  for these mixtures. According to Ronney and Wachman [33], the burning velocities are identical at one-g and zero-g when  $S_u^0 > 15$  cm/s. Simulation results in Fig. 1 for CH<sub>4</sub>/air at NTP indicate that  $S_u^0 > 15$  cm/s when  $0.7 \leq \phi \leq 1.4$ . Therefore, the contribution of buoyancy to the discrepancies in  $S_u^0$  is negligible for CH<sub>4</sub>/air with  $0.7 \leq \phi \leq 1.4$ . For  $\phi = 0.6$ , this effect to the discrepancies in  $S_u^0$  is not quantified. Nevertheless, for this equivalence ratio of  $\phi = 0.6$ , significant discrepancy in  $S_u^0$  is probably mainly caused by uncertainty in the equivalence ratio (discussed in Section 4.1) rather than buoyancy.

### 4.4. Instability

Compared to the constant-volume OPF method, the constant-pressure OPF method has the advantage that the propagating flame surface is observed such that instability that might develop over the flame surface during its propagation can be revealed. In OPF experiments, the flame propagation speed can be enhanced by thermal-diffusive and hydrodynamic instabilities. Therefore, the upper bound,  $R_{fl}$ , should be properly chosen to make the flame propagation speed devoid of instability effect [36].

Thermo-diffusive flame front cellular instability develops for mixtures with negative Markstein length or sub-unity Lewis number (e.g., [37]). For CH<sub>4</sub>/air at NTP, Fig. 2 shows that the Markstein length is positive. Therefore,  $S_u^0$  measured for CH<sub>4</sub>/air at NTP using the OPF method is almost unaffected by thermal-diffusive instability. Hydrodynamic instability usually develops as the ratio between flame thickness and flame radius decreases (e.g. at high pressure) [37]. For CH<sub>4</sub>/air at NTP and flame radius below 3 cm, the hydrodynamic instability does not occur in OPF [17]. Therefore, there is negligible contribution of flame instability to the discrepancies in  $S_u^0$  measured for CH<sub>4</sub>/air at NTP using the OPF method.

### 4.5. Confinement

In previous studies on  $S_u^0$  measurement using the OPF method [13–26], the burned gas was assumed to be static (i.e.  $u_b = 0$ ; and  $u_b$  is the flow speed of burned gas close to the flame front). For OPF in a confined chamber, a negative flow velocity of burned gas can be induced as the flame size increases [38–41]. Therefore, the assumption of zero burned gas velocity fails at relative large value of  $R_f/R_W$  ( $R_W$  is the inner radius of a spherical chamber or equivalent radius,  $R_W = (3V/4\pi)^{1/3}$ , for a non-spherical chamber of volume  $V$ ), leading to reduction in  $S_u^0$  from its correct value [38].

The normalized inward flow velocity of burned gas for OPFs of CH<sub>4</sub>/air in confined spherical chambers with different radii is shown in Fig. 8. In simulation,  $u_b$  is the minimum flow speed and it is very close (the relative difference is within 0.5%) to the flow speed at the position where 99.9% of the total heat release occurs. It is observed that  $|u_b/S_b^0| < 1\%$  for  $R_f/R_W < 25\%$ , above which  $|u_b/S_b^0|$  increases significantly. Since  $|u_b|$  increases as the stretch rate (which is inversely proportional to  $R_f$ ) decreases, the confinement effect is magnified after linear extrapolation to zero stretch rate to get  $S_b^0$  and  $S_u^0$ . Consequently, Fig. 9 shows that the relative reduction in  $S_u^0$  caused by confinement effect is still around 2–3% even when spherical flames with  $R_f/R_W < 25\%$  is used in linear extrapolation. According to Table 1, in most of previous studies [13–16,19–22,24,25], the upper bound,  $R_{fl}$ , chosen in data processing is less than 25% of the (equivalent) chamber radius,

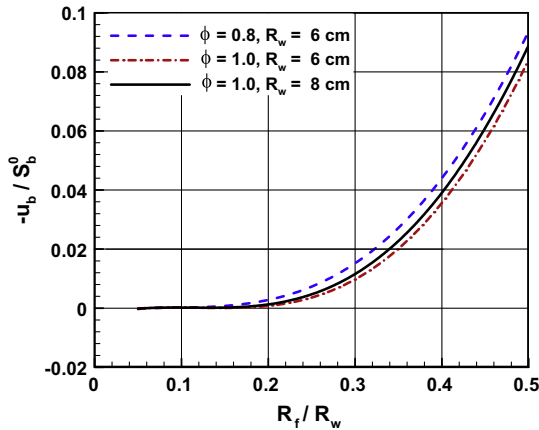


Fig. 8. Normalized inward flow velocity of burned gas in propagating spherical CH<sub>4</sub>/air flames at NTP.  $R_w$  is the inner radius of the spherical chamber.

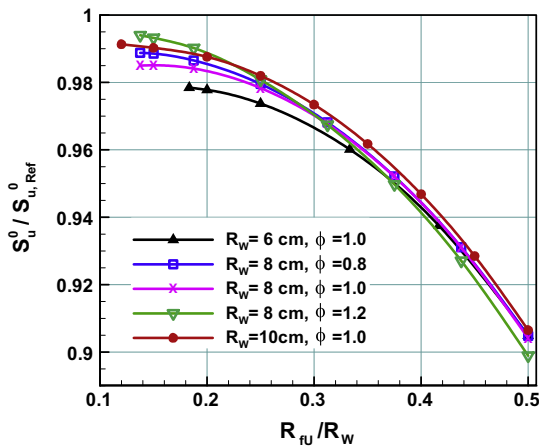


Fig. 9. Normalized laminar flame speed extrapolated using different flame radius ranges,  $[R_{fl}, R_{fu}]$ , for CH<sub>4</sub>/air at NTP.  $R_w$  is the chamber radius and  $R_{fl} = 0.1R_w$ .  $S_{u,Ref}^0$  is obtained from the corresponding OPFs with  $R_{fl} = 1$  cm,  $R_{fu} = 2$  cm, and  $R_w = 100$  cm and thereby it is not affected by confinement effect.

and thereby the confinement-induced reduction in  $S_u^0$  is within 3%. Nevertheless, for some studies using relatively smaller chamber [17,18,23,26], the confinement-induced reduction in  $S_u^0$  might be larger than 3% and flow correction [38,39] needs to be used to reduce the influence of confinement.

#### 4.6. Radiation

While radiation effect was always neglected in previous experiments [13–26], spherical flame propagation is inherently affected by radiation. It has been found that radiation has two effects on spherical flame propagation [41]: (1) a radiation-induced thermal effect by which flame temperature and thus spherical flame propagation speed is reduced; and (2) a radiation-induced flow effect by which flame propagation speed is reduced due to the inward flow of burned gas generated by radiation cooling. Therefore, radiation can lead to reduction of  $S_u^0$  from its correct value [9,10,41–44]. Recently, Yu et al. [44] have quantified the radiation-induced reduction in  $S_u^0$  measured from the OPF method.

The normalized  $S_u^0$  from OPF with radiation (see [44] for details) is plotted in Fig. 10 as a function of equivalence ratio for CH<sub>4</sub>/air at NTP. Since the linear behavior between  $S_b$  and  $K$  maintains for both adiabatic and radiative cases when the flame radius is not too large

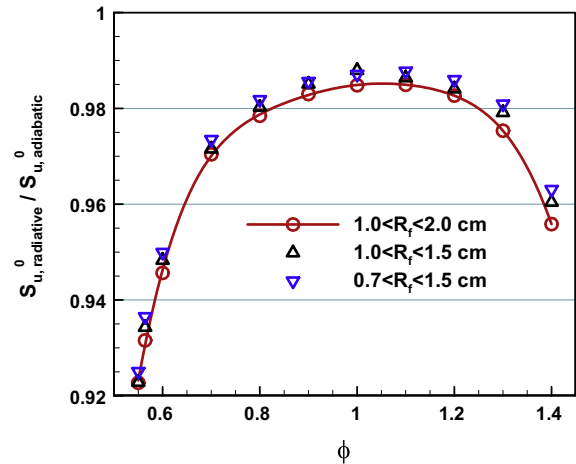


Fig. 10. Radiation effect on laminar flame speed obtained from propagating spherical CH<sub>4</sub>/air flames at NTP.

[44], the results in Fig. 10 are based on laminar flame speeds extracted from linear extrapolation according to Eq. (1). It is noted that the simulation results depend on radiation model and here the SNB (statistical narrow band) model [42] is used. The radiation-induced reduction in  $S_u^0$  is shown to be within 3% for  $0.7 \leq \phi \leq 1.3$ , and it becomes around 5% and 4% for  $\phi = 0.6$  and  $\phi = 1.4$ , respectively. For near lean flammability mixture with  $0.5 < \phi < 0.6$ , the radiation-induced reduction in  $S_u^0$  is above 6%. Therefore, the contribution of radiation to the discrepancies in  $S_u^0$  (measured for CH<sub>4</sub>/air at NTP using the OPF method) strongly depends on the equivalence ratio. Besides, Fig. 10 indicates that the influence of radiation slightly depends on the flame radius range used in data processing: the radiation-induced reduction in  $S_u^0$  decreases when OPFs with smaller radii are considered in linear extrapolation. This is reasonable since the radiation-induced flow effect increases with flame radius [44].

It is noted that Jayachandran et al. [10] showed that the error associated with radiation-induced flow effect can be avoided through direct flow and flame front speed measurements with high-speed PIV [25,77,78]. Nevertheless, in such measurements the effect of heat loss through particle radiation and conduction and the uncertainty in flow speed measurement may also affect the accuracy of laminar flame speed measured from the OPF method.

#### 4.7. Nonlinearity

In the OPF method, both linear model (Eq. (1) or Eq. (2)) and nonlinear model (Eq. (3)) can be used in extrapolation of unstretched laminar flame speed. It has been found that for mixtures with Lewis number appreciably different from unity (large absolute value of Markstein length), nonlinear stretch behavior occurs [22,45–49] and the nonlinear model in Eq. (3) helps to get more accurate extrapolation results than the linear model. (For mixtures with small Lewis number or negative Markstein length, e.g. lean H<sub>2</sub>/air, recent studies [48,49] have demonstrated that  $S_u^0$  might be under-predicted by more than 50% using the linear model. Fortunately, as shown in Fig. 2, the Markstein length of CH<sub>4</sub>/air at NTP is positive.)

Figure 11 compares the results extrapolated using linear and nonlinear models. It is observed that under fuel-lean and stoichiometric conditions, the nonlinear stretch behavior has little influence (within 2%) on  $S_u^0$ . However, for fuel-rich cases with  $\phi = 1.3$  and  $\phi = 1.4$ , the relative difference between results extrapolated

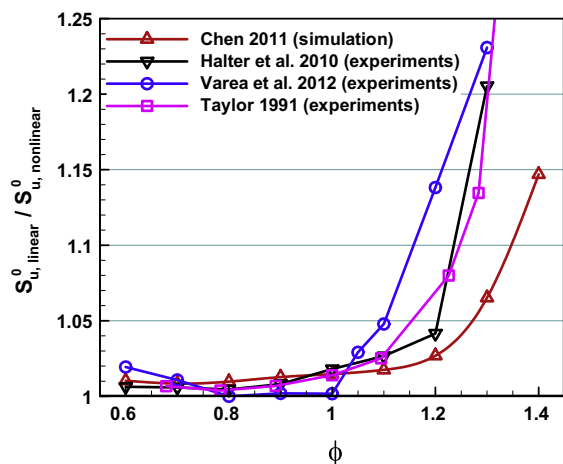


Fig. 11. Comparison between extracted laminar flame speeds from linear and nonlinear models for CH<sub>4</sub>/air flames at NTP.

using linear and nonlinear models is above 5% and can even reach 15%. (It is noted that the relative difference also depends on the flame radius range used in extrapolation [22,46].) Therefore, there is small (within 2%) contribution of nonlinearity between  $S_b$  and  $K$  to the discrepancies in  $S_u^0$  measured for CH<sub>4</sub>/air with  $\phi \leq 1.0$  and this contribution becomes larger at higher equivalence ratio.

#### 4.8. Extrapolation

Since sphere flame propagation at small and large radii is affected differently by those factors discussed above, the choice of flame radius range used for extrapolation,  $[R_{fl}, R_{fu}]$ , is another influential component which affects  $S_u^0$  measured using the OPF method [50,51].

It has been found that for mixtures with large Markstein length (large Lewis number), the extracted laminar flame speed strongly depend on the model and flame radius range used in extrapolation. However, for mixtures with small Markstein length (Lewis number close to unity), the effects of extrapolation model and flame radius range are negligible [50]. This is confirmed by results in Fig. 12, which plots the extrapolated  $S_b^0$  using experimental data for CH<sub>4</sub>/air from Taylor [13]. It is noted that the Markstein length for  $\phi = 1.4$  is much larger than that for  $\phi = 1.0$  (Fig. 2). Therefore, Fig. 12 shows that for  $\phi = 1.0$ , neither the extrapolation model nor the flame radius range has obvious influence on the extracted results. However, for  $\phi = 1.4$ , the extracted  $S_b^0$  strongly depends on flame radius range and extrapolation model: the relative difference in  $S_b^0$  extracted from different flame radius ranges can be above 20% when the linear model is used. Compared to linear model, the use of nonlinear model is shown to yield extracted  $S_b^0$  that is more consistent and less sensitive to flame radius. Therefore, when the linear model is used, the choice of flame radius range used in extrapolation has small contribution to the discrepancies in  $S_u^0$  measured for CH<sub>4</sub>/air with  $\phi \leq 1.0$  but its contribution becomes larger at higher equivalence ratio.

Table 2 summarizes the contributions of different factors to the uncertainty of measured  $S_u^0$  for CH<sub>4</sub>/air at NTP using the OPF method.

#### 4.9. Other possible sources

It is noted that it is hard to give a complete list of all sources of uncertainty and that some sources can be missing. As suggested by one of the anonymous reviewers, there are two other sources that

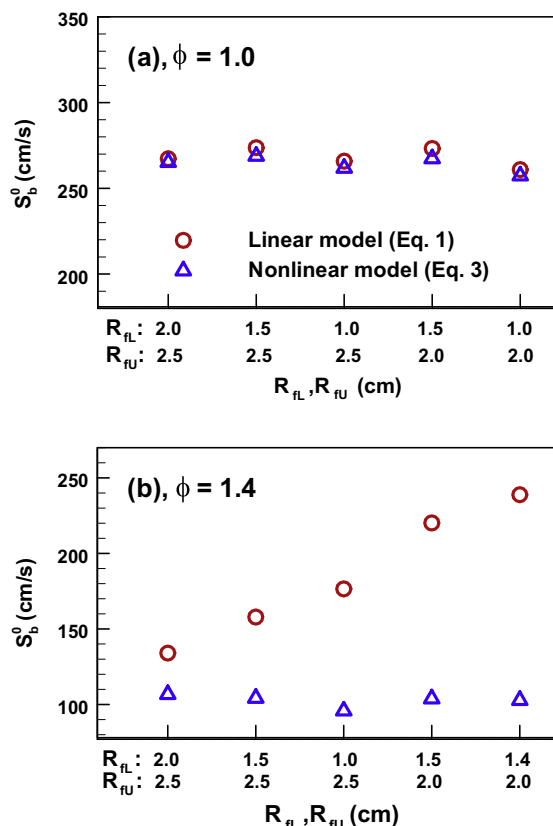


Fig. 12. Extracted laminar flame speeds from different radius ranges,  $[R_{fl}, R_{fu}]$ , for CH<sub>4</sub>/air flames at NTP. The data utilized for extraction are experimental results from Taylor [13] for methane/air mixtures.

might contribute to the uncertainty of  $S_u^0$  measurement using the OPF method.

The spherical flame front can be defined or identified at different iso-contours when different techniques such as schlieren or shadowgraphy are used to record the flame propagation. For CH<sub>4</sub>/air at NTP, our simulation results indicate that  $S_u^0$  is not affected by the isotherm chosen in data processing. The same conclusion was also drawn in the work of Bradley et al. [29] (see Fig. 5 in that paper). It is noted that unlike  $S_u^0$ , the value of Markstein length strongly depends on the isotherm chosen in data processing.

The spatial and temporal resolution of the high-speed camera used in OPF experiments might also affect the accuracy of  $S_u^0$  measurement. The spatial resolution of the camera is usually within 0.1 mm/pixel and the flame front is usually obtained from the images recorded by high-speed camera using an automated detection program for ease of processing and reduction of human bias. Therefore, the error due to spatial resolution of the camera is negligible. For CH<sub>4</sub>/air flame at NTP, the propagation speed is less than 250 cm/s and enough data can be recorded even at a low camera frame rate of 2500 frames/s. Consequently, there is little influence of camera speed (frame rate) on  $S_u^0$  measured for CH<sub>4</sub>/air at NTP using the OPF method. For fast propagating spherical flames (e.g., H<sub>2</sub>/air or syngas/air flames or flames at elevated temperature), camera operating at high frame rate should be used so that enough data points are recorded and available for data processing.

It is noted that for some equivalence ratios, these effects (listed in Sections 4.1–4.9) might appear insufficient to explain the large discrepancies in  $S_u^0$  measurement shown in Figs. 1 and 3. There might exist other sources of uncertainty/inaccuracy which deserve further study. Besides, the present work only examine the

**Table 2**  
Different factors affecting the uncertainty of laminar flame speed measured using the OPF method.

No.	Factors	Contributions to the uncertainty of $S_u^0$ measured for CH <sub>4</sub> /air at NTP using the OPF method	Notes <sup>a</sup>	References
1a	Initial $P$ and $T_u$	Negligible contribution from $P$ ; around 2% for $\Delta T_u = \pm 3$ K; around 2.5–4% for $\Delta T_u = \pm 5$ K	P0, T0, NO	[5,9,27,28]
1b	Composition (uncertainty in $\phi$ )	About 6% for $\phi = 0.6$ and $\phi = 1.4$ when pressure gauge with high accuracy of $\pm 0.05\%$ is used; significant discrepancy (above 10%) might be caused when pressure gauge with normal or low accuracy of $\pm 0.25\%$ is used	P+, T0, N+	[5,9,27,28]
2	Ignition	Negligible contribution when $R_{fl} \geq 6$ mm	P–, T–, N+	[29–32]
3	Buoyancy	Negligible contribution for $0.7 \leq \phi \leq 1.4$	T–, N+	[33,34]
4	Instability	Negligible contribution.	P+, T0, NO	[35–37]
5	Confinement	Within 2–3% for $R_f/R_w < 25\%$ ; relatively large contribution when $R_w$ is less than 8 cm	P0, T0, NO	[38–41]
6	Radiation	Within 3% for $0.7 \leq \phi \leq 1.3$ ; around 5% for $\phi = 0.6$ and $\phi = 1.4$ ; above 6% for near lean flammability mixture ( $0.5 < \phi < 0.6$ )	P+, T–, NO	[9,10,41–44]
7	Nonlinear stretch behavior	Within 2% for $\phi \leq 1.0$ ; large contribution at high $\phi$ (it can be above 10% for $\phi = 1.4$ )	P–, T0, N+	[22,45–49]
8	Extrapolation (flame radius range)	Within 3–5% for $\phi \leq 1.0$ ; large contribution at high $\phi$ (it can be above 20% for $\phi = 1.4$ ) when the linear model is used	P–, T0, N+	[50,51]

<sup>a</sup> P0, T0, and N0 respectively indicate that the effect/contribution is nearly (not exactly) independent of initial pressure, initial temperature, and fuel carbon number (e.g. C<sub>n</sub>H<sub>2n+2</sub> for alkane); P+, T+, and N+ respectively indicate that the effect/contribution becomes larger at higher initial pressure, higher initial temperature, and higher fuel carbon number; and P–, T–, and N– respectively indicate that the effect/contribution becomes larger at lower initial pressure, lower initial temperature, and lower fuel carbon number.

individual contributions of several different sources of uncertainty. There is certainly an interdependence of the source of uncertainty which can be very complicated. As a shortcoming of the present work, the interdependence is not discussed and it should also deserve further study.

## 5. Additional notes

### 5.1. Different initial temperatures, pressures, and fuels

In the previous section we only consider CH<sub>4</sub>/air at NTP. Currently the OPF method is popularly used to measure  $S_u^0$  for different fuels at different initial temperatures and pressures. In this subsection we describe how the influence of different sources of uncertainty changes with initial pressure, initial temperature, and fuel carbon number.

At higher initial pressure, the flame thickness and Markstein length both become smaller. Therefore, the influence of ignition, nonlinear stretch behavior, and extrapolation decreases with the increase of the initial pressure. This indicates that at sub-atmospheric pressure conditions, caution should be paid to ignition and extrapolation which could cause great uncertainty of  $S_u^0$  measurements. Since the flame propagates slower and the density becomes larger at high initial pressure, the influence of buoyancy and that of radiation both increase with the initial pressure. At higher pressure, the flame becomes thinner and hydrodynamic instability develops at smaller flame radius. Therefore, the influence of instability becomes stronger at higher initial pressure. Furthermore, at higher pressure, the leakage of premixed gas in the closed combustion chamber becomes more severe and thus the influence of mixture preparation becomes stronger.

At higher initial temperature, the mixture is more easily to be ignited and the flame propagates faster. Therefore, the influence of ignition, buoyancy, and radiation decreases with the increase of the initial temperature. Since flame instability and normalized compression-induced inward flow depends weakly on the initial temperature, the influence of instability and confinement remains nearly unchanged with the initial temperature. The change of Markstein length with the initial temperature is also small and so is the influence of nonlinear stretch behavior and extrapolation.

For fuels with larger carbon number, the uncertainty in  $S_u^0$  caused by mixture composition is much more significant. It is because the uncertainty in  $\phi$  is nearly proportional to carbon number  $n$ , as indicated by Eq. (4). Besides, for liquid fuels, the heating and vaporization of fuels also bring uncertainty in the mixture composition. With the increase of fuel carbon number, fuel mass diffusivity decreases; and thus the effective Lewis number and Markstein length both increase for fuel-lean mixtures. Consequently, the influence of ignition, nonlinear stretch behavior, and extrapolation becomes stronger for fuels with larger carbon number [10]. The influence of buoyancy and radiation strongly depends on the flame propagation speed, which does not strongly depend on fuel carbon number. Therefore, the influence of buoyancy and radiation does not change greatly with fuel carbon number.

The change of influence of different sources of uncertainty with initial pressure, initial temperature, and fuel carbon number is also summarized in Table 2.

### 5.2. Direct comparison to eliminate extrapolation error

For mixtures with Lewis number appreciably different from unity, the extracted laminar flame speed strongly depends on the model and flame radius range used in extrapolation; while different extrapolations might be conducted by different researchers. Therefore, extrapolation might lead to great discrepancy in  $S_u^0$  measurement using the OPF method [10,48–51]. Recently, Jayachandran et al. [10,51] and Varea et al. [49] have suggested to directly compare the measured quantities instead of extrapolated ones with 1-D simulation results predicted by kinetics so that the uncertainty associated with extrapolation can be eliminated.

Figures 13 and 14 shows the comparison among experimental data reported in the literature and present simulation results for 1-D propagating spherical CH<sub>4</sub>/air flames at NTP with  $\phi = 0.8, 1.0,$  and  $1.2$ . It is observed in Fig. 13 that the discrepancy in  $S_b$  at a given flame radius (e.g.  $R_f = 1$  or 2 cm) measured by different research groups can be much larger than the discrepancy in  $S_b^0$  (or  $S_u^0$ ) obtained from linear extrapolation. This indicates that extrapolation might help to hide the discrepancy in raw experimental data. Therefore, on one hand, extrapolation might bring great uncertainty in  $S_u^0$  measurement; on the other hand,

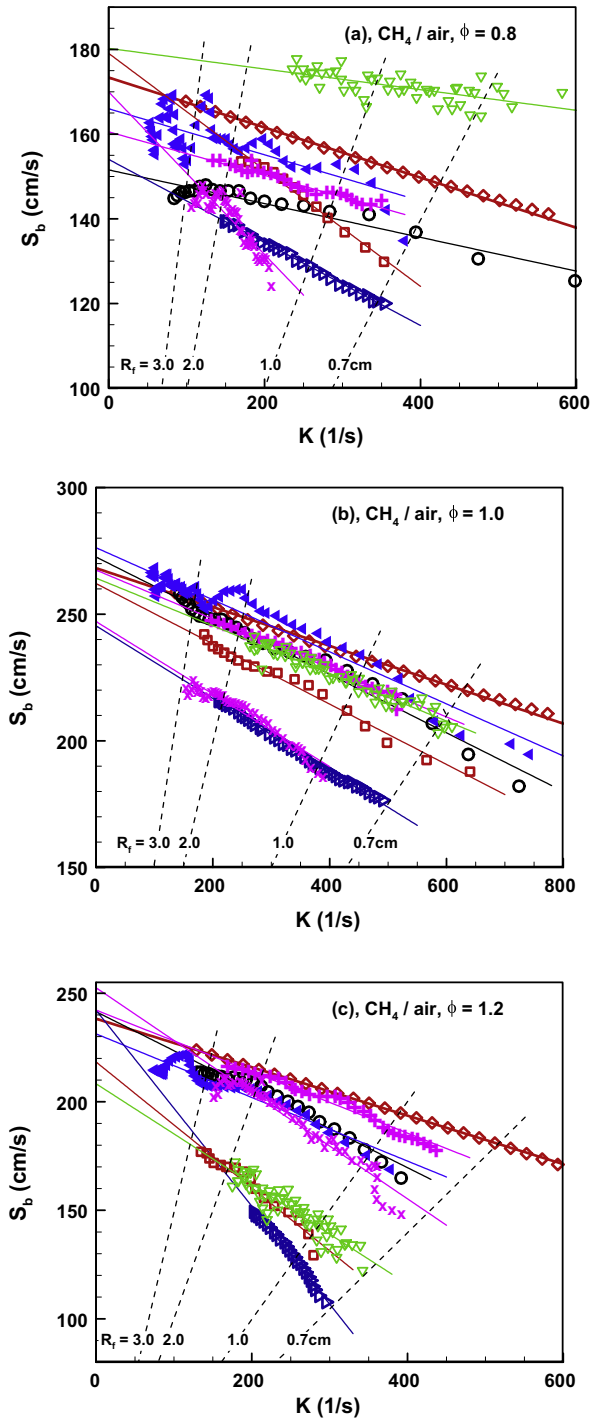


**Fig. 13.** Stretched flame speed as a function of stretch rate for propagating spherical CH<sub>4</sub>/air flames at NTP. The symbols denote simulation results (red diamond) or experimental data in the literature [13,16,19,20,22,25,30]. The solid lines stand for linear fitting and the dashed lines denote the flame radii contours (they are straight lines since  $R_f = 2S_b/K$ ). It is noted that the experimental data of Taylor [13] (black circle) are for  $\phi = 0.7835$  and  $\phi = 1.2257$  instead of  $\phi = 0.8$  and  $\phi = 1.2$ . It should be also mentioned that the experimental data of Huang et al. [30] (pink cross) are for natural gas instead of pure methane. (For interpretation of the references to color in this figure legend, the reader is referred to the web version of this article.)

large discrepancy in raw experimental data for  $S_b$  cannot be identified after extrapolation. In order to remove the complication caused by extrapolation, not only the extracted results of  $S_u^0$ , but also the data used for extrapolation ( $S_b$  versus  $K$  or  $R_f$ ) should be

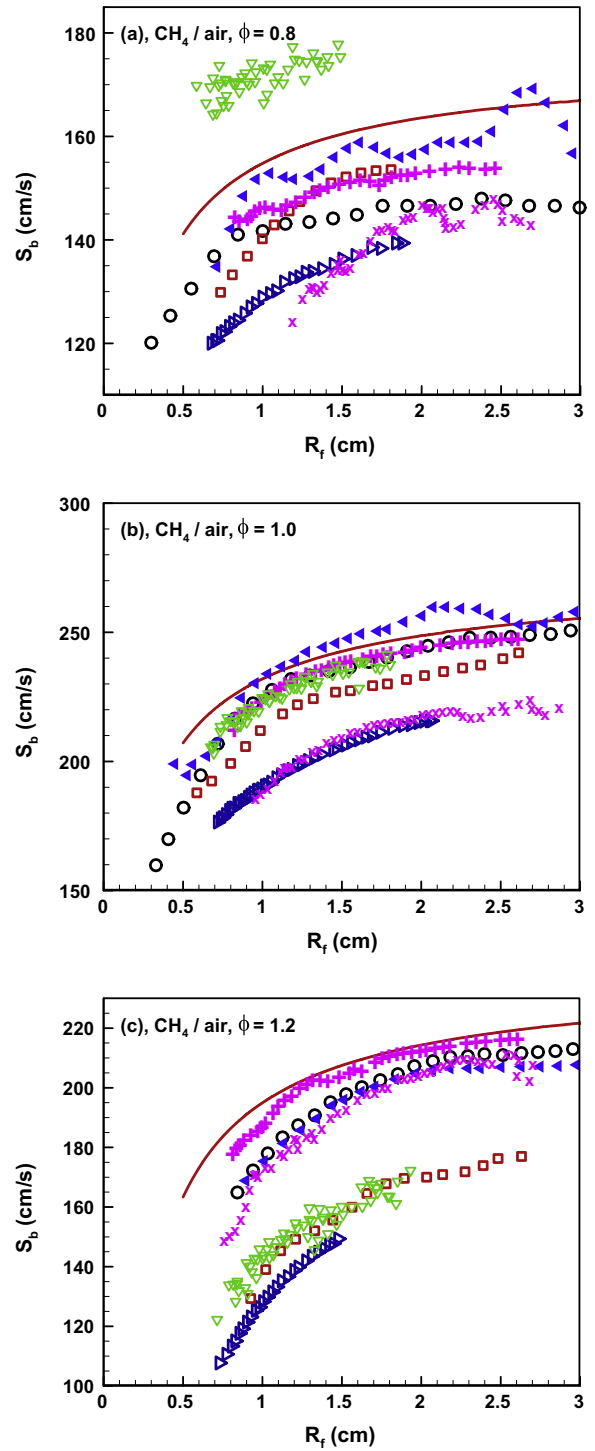


**Fig. 14.** Stretched flame speed as a function of flame radius for propagating spherical CH<sub>4</sub>/air flames at NTP. The line stands for simulation results and the symbols are experimental data in the literature [13,16,19,20,22,25,30]. It is noted that the experimental data of Taylor [13] (black circle) are for  $\phi = 0.7835$  and  $\phi = 1.2257$  instead of  $\phi = 0.8$  and  $\phi = 1.2$ . It should be also mentioned that the experimental data of Huang et al. [30] (pink cross) are for natural gas instead of pure methane. (For interpretation of the references to color in this figure legend, the reader is referred to the web version of this article.)

compared during the validation of a chemical mechanism or an experimental equipment designed for  $S_u^0$  measurement using the OPF method. This point was first proposed by Jayachandran et al. [10,51]. The same suggestion was also made by Varea et al. [49].

It is noticed that in experimental studies using the OPF method to measure  $S_u^0$ , the stretched flame speed as a function of flame radius or stretch rate is seldom reported. Therefore, it is suggested that not only the extracted results ( $S_b^0$  or  $S_u^0$ ) but also the data used for extrapolation ( $S_b$  versus  $K$  or  $R_f$ ) should be reported in future studies.

## 6. Recommendations

The present study shows that there are large discrepancies in  $S_u^0$  measured for CH<sub>4</sub>/air at NTP using the OPF method and that these data cannot be used to restrain the uncertainty of chemical models for methane. However, this does not mean that the laminar flame speed data or the OPF method is useless: they are still useful for conditions at which the uncertainty of chemical model is larger than that of  $S_u^0$  measurements.

Wang et al. [79] showed that in terms of laminar flame speed prediction, the uncertainty of chemical models increase greatly with pressure. At high pressures, the uncertainty in  $S_u^0$  measured from experiments could be lower than that of chemical models. Since OPF method has the advantage of providing  $S_u^0$  at high pressures, data from high-pressure OPF experiments can be used to restrain the uncertainty of chemical models. For examples, Burke et al. [6] measured the laminar flame speeds of hydrogen at high pressures (up to 25 atm) using the OPF method and these data were popularly used in the improvement of hydrogen mechanism [8]; Ju and coworkers [27,80–82] examined the chemical mechanisms of several hydrocarbon fuels based on  $S_u^0$  measured at high pressures using the OPF method. Besides, the laminar flame speeds at elevated temperatures are also useful for mechanism development. For example, the hydrogen mechanism was improved using the laminar flame speeds at elevated temperatures in the very recent study [83]. Therefore, it is recommended to use the OPF method to measure the laminar flame speeds at high pressures/temperatures and for fuels whose mechanisms are not well developed. Under such conditions, the uncertainty in laminar flame speed measurements can be lower than that of chemical models; and thereby data from OPF experiments can be used to restrain the uncertainty of chemical models.

On the other hand, some strategies can be taken to reduce the uncertainties in  $S_u^0$  measurements using the OPF method. Since the influence of ignition, nonlinear stretch behavior, and extrapolation becomes stronger for mixtures with large absolute value of Markstein length (i.e., the effective/global Lewis number is appreciably different from unity), the uncertainty induced by these factors can be reduced by set the mixture Lewis number close to unity (through replacing some of nitrogen by helium to increase the mixture Lewis number or by carbon dioxide to reduce the mixture Lewis number), for which the absolute value of Markstein length/number approaches zero [48]. However, if the same kinetics cannot be investigated for a mixture with Lewis number closer to unity, it is necessary to minimize the ignition and nonlinear stretch effects on the extraction of laminar flame speed. With regard to minimizing ignition/transient effects, it would be most desirable to perform multiple experiments for the same mixture conditions at different ignition energies. The flame radius, at which the flame speed vs. flame radius trajectories from different experiments converge onto the same low-dimensional manifold, would indicate the flame radius for which the flame enters the quasi-steady regime. This flame radius can then be used as the lower limit for extrapolation,  $R_{fl}$ . With regard to minimizing errors to the extrapolation models at small flame radii, for supra-unity Lewis number mixtures it would be most desirable to use linear extrapolation of the stretched flame speed based on flame curvature (i.e.  $S_b = S_b^0(1 - 2L_b/R_f)$ ) which yields extracted flame properties that are the most

accurate and least sensitive to flame radius range [50,46,48]; while for very low Lewis number mixtures, the linear and nonlinear extrapolation modes do not work [48,49] and the experimental data of  $S_b$  versus  $K$  or  $R_f$  should be reported and compared with simulation. Since the influence of buoyancy and radiation becomes stronger for mixtures with smaller propagation speeds, the uncertainty induced by these two factors can be reduced by properly adjusting the oxygen/nitrogen ratio so that the flame propagates fast enough. It is noted that spherical flame should not propagate too fast, which is constrained by the temporal resolution of the high-speed camera. In order to reduce the uncertainty caused by confinement effect, a large chamber can be used. However, compared to a smaller one, a larger chamber has the disadvantages in operational safety and cost, especially at high pressures. In order to avoid the flame instability, helium is popularly added into the mixture. Perhaps the most difficult part is to reduce the uncertainty in the mixture composition (i.e., the equivalence ratio). Pressure gauge (or mass flow meter) with high accuracy should be used when the partial pressure method (or mass flow based method) is used to prepare the mixture. Besides, great caution should be paid to heating and vaporization of liquid fuels.

## 7. Conclusions

The accuracy of  $S_u^0$  measured for CH<sub>4</sub>/air at NTP using the OPF method is investigated. Experimental data reported in the literature [13–26] are collected to show the discrepancies in  $S_u^0$  measurement. Different sources of uncertainty/inaccuracy in  $S_u^0$  measurement using the OPF method are reviewed and their contributions are assessed with the help of 1-D simulation. The main conclusions are:

1. Variety of data sets reported in the literature demonstrates that even for CH<sub>4</sub>/air at NTP, there are large discrepancies in  $S_u^0$  measured using the OPF method: the maximum difference is above 20% for  $\phi \leq 0.9$  and  $\phi \geq 1.2$ . The sensitivity-weighted uncertainty momentum of  $S_u^0$  is smaller than the discrepancies in  $S_u^0$  measurement. Therefore,  $S_u^0$  data with such large discrepancies cannot be used to restrain the uncertainty of chemical models. Significant efforts still need to be devoted to improving the accuracy of  $S_u^0$  measurement.
2. The contributions of different factors to the uncertainty of  $S_u^0$  measured using the OPF method for CH<sub>4</sub>/air at NTP are summarized in Table 2. The small difference in initial pressure and temperature, ignition, instability, and confinement have negligible contribution when proper flame radius or chamber size is used in extrapolation. Buoyancy and radiation have small contribution (within 3%) for  $0.7 \leq \phi \leq 1.3$  and their contributions increase greatly when the lean or rich flammability limit is approached. The model (linear or nonlinear model) and flame radius range used in extrapolation have small contribution (within 5%) for  $\phi \leq 1.0$  and their contributions becomes very large (above 10%) for very rich mixtures (e.g.  $\phi = 1.4$ ). Therefore, for fuel-rich CH<sub>4</sub>/air mixtures at NTP, the large discrepancies in  $S_u^0$  measurement could be partly caused by nonlinearity and extrapolation. Compared to other factors, the uncertainty in  $\phi$  contributes most to the discrepancies in  $S_u^0$  measurement, at least for off-stoichiometric mixtures with  $\phi < 0.8$  or  $\phi > 1.2$  and for experiments using pressure gauge with normal accuracy of  $\pm 0.25\%$  (this becomes even worse for larger hydrocarbon fuels).
3. For mixtures with Lewis number appreciably different from unity, extrapolation can bring great uncertainty in  $S_u^0$  measurement.

Meanwhile, large discrepancy in raw experimental data can be possibly hidden after extrapolation is conducted. Therefore, not only the extracted results of  $S_u^0$ , but also the data used for extrapolation ( $S_b$  versus  $K$  or  $R_f$ ) should be reported and compared with simulation or other experiments.

- The change of influence of different sources of uncertainty with initial pressure, initial temperature, and fuel carbon number is discussed and also summarized in Table 2. Moreover, in Section 6 we recommend to use the OPF method to measure the laminar flame speeds at high pressures/temperatures and for fuels whose mechanisms are not well developed and provide some strategies to reduce the uncertainties in  $S_u^0$  measurements using the OPF method.

## Acknowledgments

The work was supported by National Natural Science Foundation of China (Nos. 51322602 and 51136005). We thank Professor Yiguang Ju, Dr. Fujia Wu, and Mr. Jeffrey Santner at Princeton University for helpful discussions. We also thank Dr. Erjiang Hu at Xi'an Jiaotong University for providing their experimental data in [20].

## References

- G.E. Andrews, D. Bradley, *Combust. Flame* 18 (1972) 133–153.
- C.K. Law, C.J. Sung, H. Wang, T.F. Lu, *AIAA J.* 41 (2003) 1629–1646.
- S. Dooley, S.H. Won, M. Chaos, J. Heyne, Y.G. Ju, F.L. Dryer, K. Kumar, C.J. Sung, H.W. Wang, M.A. Oehlschlaeger, R.J. Santoro, T.A. Litzinger, *Combust. Flame* 157 (2010) 2333–2339.
- E. Ranzi, A. Frassoldati, R. Grana, A. Cuoci, T. Faravelli, A.P. Kelley, C.K. Law, *Prog. Energy Combust. Sci.* 38 (2012) 468–501.
- F.N. Egolfopoulos, N. Hansen, Y. Ju, K. Kohse-Hoinghaus, C.K. Law, F. Qi, *Prog. Energy Combust. Sci.* 43 (2014) 36–67.
- M.P. Burke, M. Chaos, F.L. Dryer, Y.G. Ju, *Combust. Flame* 157 (2010) 618–631.
- M.P. Burke, F.L. Dryer, Y.G. Ju, *Proc. Combust. Inst.* 33 (2011) 905–912.
- M.P. Burke, M. Chaos, Y. Ju, F.L. Dryer, S.J. Klippenstein, *Int. J. Chem. Kinet.* 44 (2012) 444–474.
- J. Beekmann, N. Chaumeix, P. Dagaut, G. Dayma, F.N. Egolfopoulos, F. Foucher, L.P.H. De Goey, F. Halter, A.A. Konnov, C. Mounaïm-Rousselle, H. Pitsch, B. Renou, E. Varea, E. Volkov, in: *Proceedings of the European Combustion Meeting*, Lund, Sweden, 2013, Paper P3-76.
- J. Jayachandran, R. Zhao, F.N. Egolfopoulos, *Combust. Flame* (2014) 2305–2316.
- D.A. Sheen, H. Wang, *Combust. Flame* 158 (2011) 2358–2374.
- X. You, T. Russi, A. Packard, M. Frenklach, *Proc. Combust. Inst.* 33 (2011) 509–516.
- S.C. Taylor, *Burning Velocity and the Influence of Flame Stretch*, Ph.D. Thesis, University of Leeds, 1991.
- K.T. Aung, L.K. Tseng, M.A. Ismail, G.M. Faeth, *Combust. Flame* 102 (1995) 526–530.
- M.I. Hassan, K.T. Aung, G.M. Faeth, *Combust. Flame* 115 (1998) 539–550.
- X.J. Gu, M.Z. Haq, M. Lawes, R. Woolley, *Combust. Flame* 121 (2000) 41–58.
- G. Rozenchan, D.L. Zhu, C.K. Law, S.D. Tse, *Proc. Combust. Inst.* 29 (2003) 1461–1470.
- X. Qin, Y. Ju, *Proc. Combust. Inst.* 30 (2005) 233–240.
- F. Halter, C. Chauveau, N. Djebali-Chaumeix, I. Gokalp, *Proc. Combust. Inst.* 30 (2005) 201–208.
- E. Hu, Z. Huang, J. He, C. Jin, J. Zheng, *Int. J. Hydrogen Energy* 34 (2009) 4876–4888.
- T. Tahtouh, F. Halter, C. Mounaïm-Rousselle, *Combust. Flame* 156 (2009) 1735–1743.
- F. Halter, T. Tahtouh, C. Mounaïm-Rousselle, *Combust. Flame* 157 (2010) 1825–1832.
- S. Wang, H. Zhang, J. Jarosinski, A. Gorczakowski, J. Podfilipski, *Combust. Flame* 157 (2010) 667–675.
- W. Lowry, J. de Vries, M. Krejci, E. Petersen, *J. Eng. Gas Turbines Power* 133 (2011) 091501.
- E. Varea, V. Modica, A. Vandel, B. Renou, *Combust. Flame* 159 (2012) 577–590.
- J. Beekmann, L. Cai, H. Pitsch, *Fuel* 117 (2014) 340–350.
- J. Santner, F.M. Haas, F.L. Dryer, Y. Ju, *Proc. Combust. Inst.* 35 (2015) 687–694.
- X. Li, X. You, F. Wu, C.K. Law, *Proc. Combust. Inst.* 35 (2015) 617–624.
- D. Bradley, P.H. Gaskell, X.J. Gu, *Combust. Flame* 104 (1996) 176–198.
- Z. Huang, Y. Zhang, K. Zeng, B. Liu, Q. Wang, D.M. Jiang, *Combust. Flame* 146 (2006) 302–311.
- Z. Chen, M.P. Burke, Y. Ju, *Proc. Combust. Inst.* 32 (2009) 1253–1260.
- H.H. Kim, S.H. Won, J.S. Santner, Z. Chen, Y. Ju, *Proc. Combust. Inst.* 34 (2013) 929–936.
- P.D. Ronney, H.Y. Wachman, *Combust. Flame* 62 (1985) 107–119.
- L. Qiao, Y.X. Gu, W.J.A. Dam, E.S. Oran, G.M. Faeth, *Proc. Combust. Inst.* 31 (2007) 2701–2709.
- S.D. Tse, D.L. Zhu, C.K. Law, *Proc. Combust. Inst.* 28 (2000) 1793–1800.
- D. Bradley, M. Lawes, K. Liu, S. Verhelst, R. Woolley, *Combust. Flame* 149 (2007) 162–172.
- G. Jomaas, C.K. Law, J.K. Bechtold, *J. Fluid Mech.* 583 (2007) 1–26.
- Z. Chen, M.P. Burke, Y. Ju, *Combust. Theory Modell.* 13 (2009) 343–364.
- M.P. Burke, Z. Chen, Y. Ju, F.L. Dryer, *Combust. Flame* 156 (2009) 771–779.
- A. Bonhomme, L. Selle, T. Poinsot, *Combust. Flame* 160 (2013) 1208–1214.
- Z. Chen, *Combust. Flame* 157 (2010) 2267–2276.
- Z. Chen, X. Qin, B. Xu, Y.G. Ju, F.S. Liu, *Proc. Combust. Inst.* 31 (2007) 2693–2700.
- J. Santner, F.M. Haas, Y.G. Ju, F.L. Dryer, *Combust. Flame* 161 (2014) 147–153.
- H. Yu, W. Han, J. Santner, X. Gou, C.H. Sohn, Y. Ju, Z. Chen, *Combust. Flame* 161 (2014) 2815–2824.
- A.P. Kelley, C.K. Law, *Combust. Flame* 156 (2009) 1844–1851.
- Z. Chen, *Combust. Flame* 158 (2011) 291–300.
- A.P. Kelley, J.K. Bechtold, C.K. Law, *J. Fluid Mech.* 691 (2012) 26–51.
- F. Wu, W. Liang, Z. Chen, Y. Ju, C.K. Law, *Proc. Combust. Inst.* 35 (2015) 663–670.
- E. Varea, J. Beekmann, H. Pitsch, Z. Chen, B. Renou, *Proc. Combust. Inst.* 35 (2015) 711–719.
- Z. Chen, Y. Wu, M.P. Burke, Y. Ju, 9th Asian-Pacific Conference on Combustion, Gyeongju, Korea, May 2013.
- J. Jayachandran, A. Lefebvre, R.H. Zhao, F. Halter, B. Renou, F.N. Egolfopoulos, *Proc. Combust. Inst.* 35 (2015) 695–702.
- M. Metghalchi, J.C. Keck, *Combust. Flame* 38 (1980) 143–154.
- K. Saeed, C.R. Stone, *Combust. Flame* 139 (2004) 152–166.
- K. Eisazadeh-Far, A. Moghaddas, J. Al-Mulki, H. Metghalchi, *Proc. Combust. Inst.* 33 (2011) 1021–1027.
- P.D. Ronney, G.I. Sivashinsky, *Siam J. Appl. Math.* 49 (1989) 1029–1046.
- G.P. Smith, D.M. Golden, M. Frenklach, et al., [http://www.me.berkeley.edu/gri\\_mech/](http://www.me.berkeley.edu/gri_mech/).
- R.J. Kee, J.F. Grcar, M.D. Smooke, J.A. Miller, Sandia National Laboratory Report SAND85-8240, 1985.
- R.J. Kee, F.M. Rupley, J.A. Miller, Sandia National Laboratory Report SAND89-8009B, 1989.
- X.L. Gou, W.T. Sun, Z. Chen, Y.G. Ju, *Combust. Flame* 157 (2010) 1111–1121.
- X.L. Gou, Z. Chen, W.T. Sun, Y.G. Ju, *Combust. Flame* 160 (2013) 225–231.
- Z. Chen, M.P. Burke, Y. Ju, *Proc. Combust. Inst.* 33 (2011) 1219–1226.
- W. Liang, Z. Chen, F. Yang, H. Zhang, *Proc. Combust. Inst.* 34 (2013) 695–702.
- Z. Chen, *Int. J. Hydrogen Energy* 34 (2009) 6558–6567.
- P. Dai, Z. Chen, S.Y. Chen, Y. Ju, *Proc. Combust. Inst.* 35 (2015) 3045–3052.
- D.A. Sheen, X. You, H. Wang, T. Lovas, *Proc. Combust. Inst.* 32 (2009) 535–542.
- D.M. Golden, *Int. J. Chem. Kinet.* 45 (2013) 213–220.
- A.P. Kelley, W. Liu, Y.X. Xin, A.J. Smallbone, C.K. Law, *Proc. Combust. Inst.* 33 (2011) 501–508.
- L.T. He, *Combust. Theory Modell.* 4 (2000) 159–172.
- Z. Chen, Y. Ju, *Combust. Theory Modell.* 11 (2007) 427–453.
- H. Zhang, Z. Chen, *Combust. Flame* 158 (2011) 1520–1531.
- H. Zhang, P. Guo, Z. Chen, *Proc. Combust. Inst.* 34 (2013) 3267–3275.
- W.K. Zhang, Z. Chen, W.J. Kong, *Combust. Flame* 159 (2012) 151–160.
- M. Nakahara, F. Abe, K. Tokunaga, A. Ishihara, *Proc. Combust. Inst.* 34 (2013) 703–710.
- M. Nakahara, F. Abe, K. Tokunaga, A. Ishihara, *Proc. Combust. Inst.* 35 (2015) 639–646.
- L. Qiao, Y. Gu, W.J.A. Dam, E.S. Oran, G.M. Faeth, *Combust. Flame* 151 (2007) 196–208.
- L. Qiao, Y. Gan, T. Nishiie, W.J.A. Dam, E.S. Oran, *Combust. Flame* 157 (2010) 1446–1455.
- S. Balusamy, A. Cessou, B. Lecordier, *Exp. Fluids* 50 (2011) 1109–1121.
- E. Varea, V. Modica, B. Renou, A.M. Boukhalfa, *Proc. Combust. Inst.* 34 (2013) 735–744.
- H. Wang, O. Park, F.N. Egolfopoulos, D. Sheen, G. Smith, in: *Multi-agency Coordination Committee for Combustion Research (MACCCR)*, Alington, VA, USA, 2013.
- D. Liu, J. Santner, C. Togbe, D. Felsmann, J. Koppmann, A. Lackner, X.L. Yang, X.B. Shen, Y.G. Ju, K. Kohse-Hoinghaus, *Combust. Flame* 160 (2013) 2654–2668.
- J. Santner, F.L. Dryer, Y.G. Ju, *Proc. Combust. Inst.* 34 (2013) 719–726.
- X. Shen, X. Yang, J. Santner, J. Sun, Y. Ju, *Proc. Combust. Inst.* 35 (2015) 721–728.
- V.A. Alekseev, M. Christensen, A.A. Konnov, *Combust. Flame* 162 (2015) 1884–1898.